Review

Metathesis polymerization-derived chromatographic supports

Michael R. Buchmeiser*

Institut für Analytische Chemie und Radiochemie, Universität Innsbruck, Innrain 52 a, A-6020 Innsbruck, Austria

Available online 21 July 2004

Abstract

The synthesis and properties of metathesis polymerization-derived supports for solid-phase extraction (SPE), for the on-line extraction of metal ions, ion-chromatography, reversed-phase (RP-) chromatography, and chiral chromatography is described. In addition, the metathesis polymerization-based manufacture and derivatization of monolithic supports and their use in the separation of biomolecules such as oligonucleotides, thiooligonucleotides, double-stranded DNA (dsDNA) and proteins will be summarized. Special consideration will be given to important aspects of polymer chemistry and their relevance to the properties of these new supports.
© 2004 Elsevier B.V. All rights reserved.

Keywords: Reviews; Stationary phases, LC; Metathesis polymerization; Solid-phase extraction; Enantiomer separation; Monolithic columns; Proteins; DNA; Metal ions

Contents

* Tel.: +43-512-507-5184; fax: +43-512-507-2677.
E-mail address: michael.r.buchmeiser@uibk.ac.at (M.R. Buchmeiser).

1. Introduction

Besides distillation, sublimation and filtration, chromatography and hyphenated techniques certainly belong to the most important tools in separation science. Their successful use is strongly related to the continuous and on-going developments in chromatographic supports. Modern separation techniques require designed, high-performance materials with regard to particle size, particle shape, porosity, specific surface area, functionality and capacity, respectively. Most chromatographic supports are based on surface-modified silica, titania, zirconia, alumina or organic polymers such as acrylates or poly(styrene-co-divinylbenzene) (PS-DVB) [1]. While derivatization reactions of silica-based materials are easy to perform and fairly easy to control, even highly sophisticated end-capping procedures are still hardly capable of overcoming the pH instability from which these materials suffer. The resulting limitations in working pH and temperature entail several problems, significantly limiting their range of applicability, in particular the use of acidic or basic substrates. While PS-DVB-based materials overcome the problem of hydrolysis, a major problem encountered with these carriers lies in rather poorly controllable surface derivatization. Consequently and despite the existence of highly sophisticated analytical tools, the nature of the "working" functionality is sometimes still based on assumption than on real analysis. In order to avoid any multi-step derivatization reactions, the polymerization of *functional monomers* therefore appeared favorable. In this context, living polymerizations techniques [2,3] are of particular interest since they allow full control over both molecular weights and architecture of the resulting polymers. This permits the stoichiometric design of block-copolymers including cross-linked polymers. These characteristics and the fact, that neither the sterical nor the conformational situation of any monomer is changed in course of the polymerization leads to high reproducibility in the synthesis of these tailor-made materials. Consequently, this facilitates the correlation between the material's structure and the resulting separation properties. The desired living polymerization of functional polymers can be accomplished by metathesis-derived polymerization techniques such as ring-opening-metathesis polymerization (ROMP) or 1-alkyne polymerization using well-defined, high-oxidation state metathesis initiators either based on molybdenum [4–8] or ruthenium [9–16]. While "Schrock-type", molybdenum-based systems represent highly active initiators, they are generally not capable of polymerizing monomers containing protic hydrogens such as alcohols, carboxylic acids or thiols. However, a broad range of functional monomers based on substituted norborn-2-enes and norbornadienes bearing anhydrides, esters or amides may be polymerized. The ruthenium-based systems developed by Grubbs et al. exhibit a higher stability towards protic functionalities compared to the molybdenum analogues. This permits the polymerization of functionalized norborn-2-enes and 7-oxanorborn-2-enes even in aqueous media. Despite these advantages, it must be stated that ruthenium-based, living polymerization systems, which are comparable to Schrock-type initiator based polymerizations in terms of quality and control, have only been reported recently [17]. In view of these particular properties, the use of both types of initiators in the synthesis of various separation media was investigated. This review provides a concise yet comprehensive summary of the developments and achievements that have been accomplished in the area of chromatographic supports prepared by metathesis polymerization-based techniques.

2. Supports for SPE prepared by ring-opening metathesis precipitation polymerization

Solid-phase extraction (SPE) has become an important tool for sample clean up and preconcentration in analytical chemistry [18,19]. Consequently, a large variety of different SPE-materials is available and has been applied successfully to different problems. In the course of our search for new pH-stable, high-capacity polymers, we developed a completely new approach towards SPE materials, combining ROMP with precipitation polymerization techniques. The new concept entailed the copolymerization of functional monomers with a suitable cross-linker, leading to polymeric, pH-stable stationary phases with both defined functionality and capacity in a reproducible way [15].

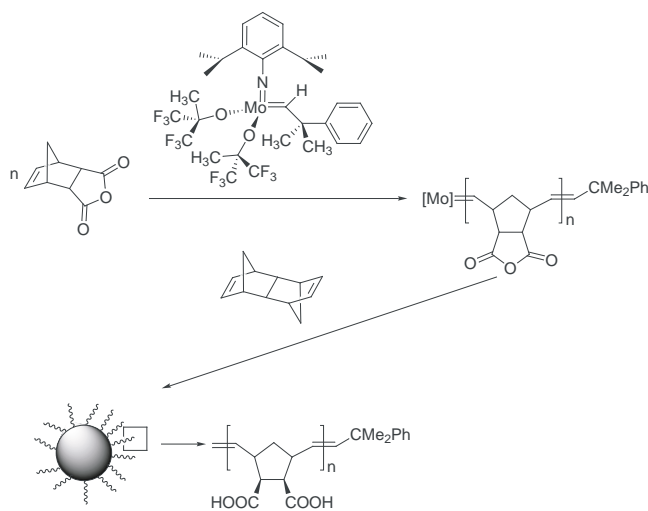### 2.1. Carboxylic acid derivatized polymers [20–23]

Suspension polymerization of norborn-5-ene-2,3-dicarboxylic anhydride in dichloromethane using Mo(N-2,6-i-Pr$_2$-C$_6$H$_3$)(CHCMe$_2$Ph)(OCMe(CF$_3$)$_2$)$_2$ as initiator yielded living, linear polymer chains with the active initiator at the polymer chain end. The solubility of poly(norborn-5-ene-2,3-dicarboxylic anhydride) strongly depends on the chain length. Oligomers containing up to approximately 10–15 monomer units are soluble, longer chains are entirely insoluble. By choosing a degree of polymerization >15 for the living oligomers, precipitation (phase separation) was induced. Addition of a cross-linker (1,4,4a,5,8,8a-hexahydro-1,4,5,8-*exo-endo*-dimethanonaphtalene = DMN-H$_6$) to the living polymers lead to a covalent attachment of these living polymer chains to the highly cross-linked matrix. The chosen polymerization order guaranteed that the linear polymer chains built from the functional monomer were attached to a cross-linked matrix in a way that they formed tentacles at the surface of the beads. The achieved *quantitative* consumption of both the functional monomer and the cross-linker met the requirements of the concept for the stoichiometric build-up of these materials. An overview over the polymers is given in Table 1. All polymerizations were end-capped using ferrocene- or benzaldehyde in order to ensure the clean removal of the molybdenum-core from the

Table 1
Selection of poly(norborn-5-ene-2,3-dicarboxylic acid)- and poly(norborn-5-ene-2-dipyridyl carbamide)-functionalized resins prepared by ring-opening metathesis precipitation polymerization [20,21,23,30,38,77]

Functional group	Ligand (mmol/g)
1,4-Butanediacid (succinic acid)	7.30
1,4-Butanediacid (succinic acid)	3.75
1,4-Butanediacid (succinic acid)	3.13
N,N-Dipyrid-2-ylcarbamide	1.0
N,N-Dipyrid-2-ylcarbamide	0.6

Average particle size: $40 \pm 10 \, \mu$m.

polymer. The synthesis and structure of the resins are shown in Scheme 1. Prior to use, all resins were transformed into the corresponding *vic*-dicarboxylic acid (polymer-bound succinic acid) by treatment with aqueous sodium hydroxide for 6 h, followed by addition of an excess of aqueous hydrochloric acid. This procedure also ensured a complete removal of molybdenum. Determination of the actual molybdenum content of the resin was carried out by means of inductively coupled plasma optical emission spectroscopy (ICP-OES) and confirmed a removal of more than 99.6% of the initial molybdenum, resulting in a final molybdenum content of the resin of less than 40 ppm. Theoretical capacities, expressed in mmol COOH/g resin, were calculated from the molar ratio of norborn-5-ene-2,3-dicarboxylic anhydride to DMN-H$_6$ and were in good accordance with the values experimentally confirmed by acid base titration (Table 1). Due to the large amounts of carboxylic acid groups located at the outer surface of these materials, they were wetted by water alone. This unique property was characteristic and in fact necessary for applications in SPE. As a consequence, no organic modifier such as methanol was required to mediate between the organic resin and water.

Scheme 1. Synthesis of carboxylic acid-derivatized polymers prepared via ring-opening metathesis precipitation polymerization.

Following this setup, a series of resins were prepared. The maximum length for the functional group containing tentacles was found to lie in the range of 50. In case longer tentacles were formed, the material started gelling upon treatment with polar solvents such as methanol, water or even diethyl ether. This finding was explained by the formation of strong hydrogen bonding caused by the long dicarboxylic acid functionalized chains concentrated at the surface of the particles. In the case where the degree of polymerization (DP) of the tentacles was >50, they became long enough to cause a strong inter-particle interaction, leading to the formation of a gel-like, solvent swollen matrix. This behavior was considered as further proof for the proposed tentacle-type structure of these resins.

The polymers prepared by the procedure described above showed a mean particle diameter of $40 \pm 10 \, \mu$m. The particle shape itself was quite irregular. The specific surface area of resins was found to be within $10–30 \, m^2/g$, which suggested a non-porous structure. Nevertheless, a non-permanent porosity due to the increase in volume in the swollen state had to be assumed. This assumption was confirmed by determining the characteristic parameters by means of inverse SEC [24,25]. Using this technique, a specific pore volume of $750 \, \mu$L/g and a specific surface area of ca. $80 \, m^2/g$ in the conditioned state were found.

2.1.1. Applications in SPE of organic compounds

The most straightforward characterization of the new resins in terms of their retention characteristics, efficiency as well as selectivity, was to investigate their interaction with various analytes in different matrices. In this context, the corresponding breakthrough curves, describing the maximum amount of each compound being held back by the resin, as well as the total recovery, describing the efficiency of elution, were of major interest. In a first step, aqueous mixtures of strong and weak amines (lutidines and anilines) [23] as well as volatile, airborne amines were investigated [26].

As can be deduced from Table 2, excellent recoveries were observed, exceeding by far commercially available silica-based SPE materials. In an extension to these investigations, the new supports were investigated for their retention behavior for phenols, alcohols, carboxylic acids, aldehydes, ketones, esters, chloroalkenes and polycyclic aromatic hydrocarbons (PAHs) [27]. To realize a construction similar to commercially available Empore discs® (3 M), the new materials were processed into Teflon sheets resulting in membranes filled with the new sorbent. Again, excellent recoveries were achieved with the carboxylic acid ROMP-derived supports (Tables 3 and 4). An additional investigation on the extraction efficiency for phenols using silica-C18, carboxypropyl silica and the new sorbents again went in favor of the latter (Table 5) [28].

Another area of interest was the retention behavior of the new materials versus volatile basic compounds. Since such volatile amines are used as accelerators in commercial

Table 2
Recoveries for anilines and lutidines on a carboxylic acid derivatized, ROMP-derived support in comparison to commercially available silica-based resins $n = 3$

Amine	500 mg silica-CO_2H[a] recovery ± σ_{n-1}[c]	50 mg ROMP-derived resin[b] recovery ± σ_{n-1}[c]
2,6-Lutidine	70 ± 6	100 ± 8.8
2,4-Lutidine	79 ± 23	103 ± 8.3
N-Methylaniline	69 ± 11	101 ± 8.0
N,N-Dimethylaniline	86 ± 6	101 ± 6.6
2-Chloroaniline	0	95 ± 6.3
2,6-Dimethylaniline	0	97 ± 6.6
3-Chloroaniline	0	63 ± 4.6
2-Nitroaniline	0	100 ± 6.5
2,6-di-2-Propylaniline	86 ± 15	102 ± 5.9
1-Naphtylamine	35 ± 4	61 ± 2.6
Diphenylamine	90 ± 9	105 ± 4.6

[a] ICT-*Bond-elut*, capacity: ca. 1 mequiv./g.
[b] 3.9 mmol COOH/g.
[c] Determined in methanol:water = 20:80 (v/v), 5 mL of mixed standard (10 ppm each).

polyurethane (PU) foams, they frequently occur during the application of PU-based products. To our pleasure, the new sorbents could again be used for the determination of such strongly basic, volatile, air born amines. Table 6 summarizes the data obtained with the new supports [26].

Finally, the materials were used as on-line cation exchangers for the suppression of adduct formation in negative-ion electrospray ionization mass spectrometry (ESI-MS) of nucleic acids [29]. In this context, one major difficulty in the analysis of nucleic acids by ESI-MS stems from the affinity of the polyanionic sugar-phosphate backbone for nonvolatile cations, especially ubiquitous sodium and potassium ions. A simple on-line sample preparation system comprising of a microflow pumping system and 45 mm × 0.8 mm i.d. microcolumns packed with the new resins was used for the efficient removal of cations from nucleic acid samples. After on-line desalting, mass spectra of oligonucleotides revealed no significant sodium adduct peaks. Moreover, signal-to-noise ratios were greatly enhanced compared to direct injection of the samples. Using this setup, ESI-MS with on-line sample preparation allowed accurate molecular mass determinations of picomole amounts of crude oligonucleotide preparations ranging in size from 8 to 80 nucleotides within a few minutes. Furthermore, quantitative measurements of oligonucleotides were possible in a concentration range of 0.2–20 mM with selected-ion monitoring.

2.1.2. Applications in the SPE of lanthanides [22,30]

Lanthanides are among the most important elements for elucidating igneous rock petrogenesis and for the interpretation of processes of metasomatism, ore formation and rock alteration [31]. In principle, rare earth elements (REEs) may be extracted from aqueous rock digests us-

ing solvent extraction. In the case of comparably low amounts of REEs ($<10 \mu g/g$) with respect to other metal ions present, separation of lanthanides is preferably performed by ion exchange procedures. These usually entail the use of preparative scale columns (e.g. 4 cm × 50 cm) filled with strong cation exchangers based on sulfonated poly(styrene-co-divinylbenzene) (PS-DVB). Such standard ion exchange separation procedures permit the concentration of REEs from large sample volumes, remove interfering compounds, reduce the total salt content and consequently significantly enhance the sensitivity of any method of quantification [32–35]. For quantification, mainly atomic absorption spectroscopy (AAS), X-ray fluorescence spectroscopy, neutron activation analysis, mass spectrometric isotope dilution analysis, and inductively coupled plasma mass spectrometry have been used [36,37]. In addition, ICP-OES has become a competitive, low cost method for REE-determination.

A modern way of enrichment is the use of polymer immobilized, complexing ligands for SPE. Unfortunately, these materials often suffer from insufficient selectivity as basically all transition metal ions and some main group elements are coextracted. Due to this unsatisfying situation and the fact that the complexation of lanthanides by various dicarboxylic acids such as oxalic or malonic acid has been known for long, we used the new polymeric material as off-line SPE materials for the selective extraction of lanthanides. ICP-OES was used for quantification. Extraction efficiencies were found to be in the range of 90–100% for REE standards containing 5 and 500 ppb of each REE, respectively. The optimum extraction pH was within narrow borders, i.e. 5.3–5.5. Three different rock standard reference materials (SRMs), GSR-1 granite, GSR-2 andesite, GSR-3 basalt, were digested by fusion of the corresponding rock with lithium metaborate ($LiBO_2$) and subsequent dissolution in nitric acid. Interfering metal ions such as Fe^{3+} and Al^{3+} were masked using 5-sulfosalicylic acid. Small amounts of methanol were added to prevent silicate from precipitation. Following this setup, REEs occurring in the digest solutions in a range of 40 ppt to 150 ppb were retained selectively with recoveries of 75–110% for most REEs. The high performance of the entire system was underlined by low relative standard deviations (R.S.D.) <10%. A summary of these data is given in Table 7.

2.2. Dipyridylamide-derivatized polymers [20,38]

Following the synthetic protocol described above, dipyridyl amide-functionalized supports suitable for SPE of metal ions from aqueous solutions were prepared. Resins were accessible via the copolymerization of the functional monomer *endo*-norborn-2-ene-5-yl-*N,N*-di-2-pyridyl carboxylic amide with DMN-H_6 using the well-defined Schrock-initiator Mo(*N*-2,6-*i*-Pr$_2$-C$_6$H$_3$)(CHCMe$_2$Ph)(OC-Me(CF$_3$)$_2$)$_2$ (Scheme 2). The polymerization of the monomer itself proceeded in a living manner, thus allowing

Table 3
Summary of recoveries (%) obtained with various SPE supports

Class	Compound	Silicalite	Empore® disc	COOH-resin[a]	COOH-membrane[b]
Phenols	Phenol	66	84	101	96
	2-Chlorophenol	33	89	101	100
	3-Nitrophenol	56	105	92	93
	2,5-Dimethylphenol	54	92	97	–
	4-Propylphenol	98	98	103	–
	4-t-Butylphenol	27	87	97	–
	m-Cresol	97	93	100	95
Alcohols	1-Pentanol	92	99	82	–
	1-Hexanol	99	91	99	–
	1-Octanol	89	94	95	100
	1-Decanol	82	89	100	93
	1-Dodecanol	75	89	83	75
	1-Tetradecanol	58	87	84	–
	3-Phenyl-1-propanol	73	99	95	–
	2-Ethyl-1-propanol	92	90	94	–
Carboxylic acids	Valeric acid	95	104	106	93
Aldehydes	Benzaldehyde	89	94	84	78
	Salicylaldehyde	54	96	92	–
	n-Valeraldehyde	100	74	89	–
	Hexanal	107	94	84	–
	Nonylaldehyde	84	96	92	–
Ketones	2-Pentanone	90	88	94	96
	4-Methyl-2-pentanone	104	88	85	92
	2-Hexanone	93	89	96	–
	3-Hexanone	81	89	93	–
Esters	Ethyl propionate	88	61	98	96
	Ethyl butyrate	90	75	108	98
	Methyl benzoate	68	94	100	–
Chloroalkanes	Chloroform	82	81	89	87
	1,2-Dichloroethane	83	77	85	78
	1,1-Dichloroethane	80	77	92	91
	1,2-Dichloropropane	85	85	92	90

pH was 2.0 for phenols and acids. Sample volumes: 10 mL; concentration: 1 ppm each analyte; sampling rate: 1 mL/min, elution with 0.5 mL acetone.
[a] 3.0 mequiv. COOH/g.
[b] 3.0 mequiv. COOH/g-resin embedded in a teflon membrane. σ_{n-1} for all compounds was 2.0%.

the stoichiometric build-up of the desired polymers. A summary is given in Table 1. Since the complexing site was neither subject to any changes in terms of connectivity nor to steric constraints during polymerization, the metal-binding abilities of the support could be studied for a large variety of mono-, di-, tri- and tetravalent metal ions on a monomeric base. This was simply accomplished by UV–Vis spectroscopy. Reaction of the *monomer* with the metal ions of interest and subtraction of the UV–Vis spectrum of the free ligand and metal ion, respectively, provided unambiguous proof for any complexation. Complementary, AAS and ICP-OES techniques were applied to confirm the results for the polymer. In contrast to dipyridyl *amines*, the polymer-bound dipyridyl *amide* ligand showed excellent selectivity toward Hg^{2+} and Pd^{2+} even under competitive conditions, allowing the selective extraction of both divalent metal ions over a broad range of concentration from complex mixtures. Due to the stability of the resulting complexes, high loadings of the material with both metals,

reaching 57 wt.%, were achieved. Again, a multiple use of the resin was possible, Thus, Pd^{2+} and Hg^{2+} could be quantitatively desorbed using thiourea in 1.5N HCl and dimercaptosuccinic acid in THF, respectively.

Generally speaking, no loss of performance was observed after recycling the new ring-opening metathesis precipitation polymerization-derived materials over more than twenty cycles. After exposure to air for at least 2 months, a change in color from bright white to yellow was observed. Nevertheless, this change in color did not influence the characteristic properties of these resins.

3. ROMP-derived stationary phases for the selective extraction of metal ions and for ion chromatography prepared by coating techniques [39]

Coating procedures for ion chromatography, e.g. the dynamic coating of n-alkyl-derivatized stationary phases with

Table 4
Recoveries (%) and relative standard deviations (σ_{n-1}) for PAHs

Compound	COOH-resin[a]	COOH-resin[b]	COOH-membrane[c]
Naphthalene	31	18.3 ± 1.5	99 ± 10.2
Acenaphthalene	82	55.6 ± 5.0	92 ± 5.2
Acenaphthene	97	77.7 ± 4.0	92 ± 6.7
Fluorene	103	94.0 ± 4.0	91 ± 6.2
Phenanthrene	103	98.7 ± 4.0	94 ± 4.2
Anthracene	97	88.0 ± 3.5	76 ± 5.0
Fluoranthene	97	94.0 ± 1.7	85 ± 4.1
Pyrene	100	93.7 ± 2.1	84 ± 3.9
Benzo[a]anthracene	99	95.0 ± 8.7	74 ± 4.5
Chrysene	87	91.3 ± 6.1	76 ± 3.2
Benzo[b]fluoranthene	94	93.0 ± 6.6	67 ± 3.2
Benzo[k]fluoranthene	94	90.7 ± 4.9	70 ± 5.7
Benzo[a]pyrene	89	89.0 ± 2.0	61 ± 3.5
Dibenzo[a,h]anthracene	82	97.3 ± 10.4	77 ± 14.2
Benzo[g,h,i]perylene	36	82.7 ± 17.2	98 ± 26.6
Indeno[1,2,3-cd]pyrene	79	100.3 ± 11.0	86 ± 14.4

COOH-resin: 3.0 mequiv. COOH/g; COOH-membrane: 3.0 mequiv. COOH/g-resin embedded in a PTFE membrane ($n = 3$).

[a] 1000 mL of compounds (1 µg/l each) in water:2-propanol 90:10. Sampling rate: 7 mL/min; elution: 2 mL ethyl acetate.
[b] 1000 mL of compounds (1 µg/l each) in water:2-propanol = 85:15. Sampling rate: 7 mL/min; elution: 2 mL ethyl acetate.
[c] 500 mL of compounds (1 µg/l each) in water. Sampling rate. Sampling rate: 3.5 mL/min; elution: 1 mL ethyl acetate.

alkyl sulfonates and alkylammonium salts, respectively, are well known [40,41]. Though easy to perform, the loss of pore volume and specific surface area entailed with such coating procedures, are major drawbacks [42]. Despite these impediments, the concept of polymer-coated inorganic or organic carriers has been further developed and improved. Coated supports may now be characterized in a very profound way and have gained interest in separation science as well as chemical sensing. Until now, optimum deposition conditions have been developed both for the hydrophobic and hydrophilic coating of silica, alumina, titania or zirconia using poly(butadiene) or poly(styrene) [1].

In view of the achievements made in this area of research, we were particularly interested in the synthesis of ROMP-derived, coated, silica-based and hence pressure stable supports carrying chelating, i.e. *vic*, *cis*-dicarboxylic acid groups. Such supports were of considerable interest

Table 5
Comparison of recoveries (%) obtained with three different materials ($n = 3$)

Compound	Carboxypropyl-silica[a] recovery	Silica-C18[b] recovery	COOH-resin[b] recovery
Phenol	12	64	101
4-Nitrophenol	13	77	98
2-Chlorophenol	26	90	95
2,4-Dinitrophenol	16	95	99
2-Nitrophenol	29	89	93
2,4-Dimethylphenol	34	95	97
4-Chloro-3-cresol	49	95	98
2,4-Dichlorophenol	52	93	95
2-Methyl-4,6-dinitrophenol	36	93	99
2,4,6-Trichlorophenol	83	90	95
Pentachlorophenol	77	66	97

pH 2.0 (silica-C18, 1000 mg), 2.2 (carboxypropyl silica, 500 mg), 1.1 (COOH-resin, 5.1 mequiv. COOH/g, 50 mg). Sample concentration: 10 µg/mL of each compound; sample volume:10 mL; flow-rate: 1 mL/min; elution: 3 mL of acetonitrile.

[a] $\sigma_{n-1} \leq 1\%$.
[b] $\sigma_{n-1} \leq 3\%$.

Table 6
Recoveries for amines after SPE from air using 50 mg carboxylic acid derivatized resin (3.75 mmol COOH/g)

Amine	Concentration (ppm (v/v))	Sampling time (min)	Recovery (%)
Pentamethyldiethylene-tetramine[a]	140	5	108
	75	10	108
	13.4	10	103
	6.8	10	108
	2.1	10	103
DABCO[a]	95	5	95
	50	5	98
	13	10	99
N-Methylmorpholine[b]	300	3	38
	120	5	68
	5	15	99
N-Ethylmorpholine[b]	170	5	87
	5	15	97
	3	15	95
Dimethylpiperazine[b]	70	5	81
	9	15	105
Dimethylethanolamine[b]	113[c]	10	108
	90	10	101
	35	10	104
	15	10	110

[a] Elution with 3 mL of Et$_3$N:MeOH = 50:50 ($n = 3$).
[b] Elution with 2 mL of NEt$_2$NH:MeOH = 50:50.
[c] 100 mg resin.

Table 7
Recoveries (%) and R.S.D. values (σ_{n-1},%) for La–Lu (without Pm) on succinic acid derivatized resin (3.1 mequiv. COOH/g, 250 mg)

Rock		La	Ce	Pr	Nd	Sm	Eu	Gd	Tb	Dy	Ho	Er	Tm	Yb	Lu
Granite	Concentration (ppb)[a]	68	135	16	59	12	1	0.04	2	13	2.6	8	1	9	1.4
	Recovery (%)	101.5	95.2	115.2	80.2	77.5	94.7	93.8	84.5	86.9	104.3	95.8	92.4	110.8	100.5
	σ_{n-1} ($n = 21$)	5.6	5.4	6.2	7.9	4.6	9.6	4.6	11.2	5.7	10.6	5.0	10.2	5.4	11.2
Andesite	Concentration (ppb)[a]	27.3	50	6.1	23.8	5.4	1.3	3.4	0.51	2.3	0.43	1.1	0.19	1.1	0.15
	Recovery (%)	120.6	94.8	103.0	85.7	90.6	89.2	79.7	[b]	93.1	[b]	[b]	[b]	86.6	[b]
	σ_{n-1} ($n = 21$)	6.6	2.7	6.7	2.8	4.0	3.0	7.8	[b]	2.4	[b]	[b]	[b]	3.0	[b]
Basalt	Concentration (ppb)[a]	70	131	17	68	12.8	4	10.6	1.5	7	1.1	2.5	0.35	1.9	0.24
	Recovery (%)	98.0	93.0	121.9	88.1	84.7	93.5	100.8	74.6	91.4	102.2	82.1	[b]	86.8	102.6
	σ_{n-1} ($n = 19$)	5.3	4.0	10.5	5.4	5.2	7.0	4.6	16.1	6.6	10.9	7.5	[b]	7.9	23.3

200 mL rock digest from 0.25 g GSR-1 granite, andesite, and GSR-3 basalt, respectively, in 0.25N nitric acid. Masking agent: 5-sulfosalicylic acid (20 g/100 mL), MeOH (0.8% (v/v), pH 5.5.
[a] Actual concentration in rock digests.
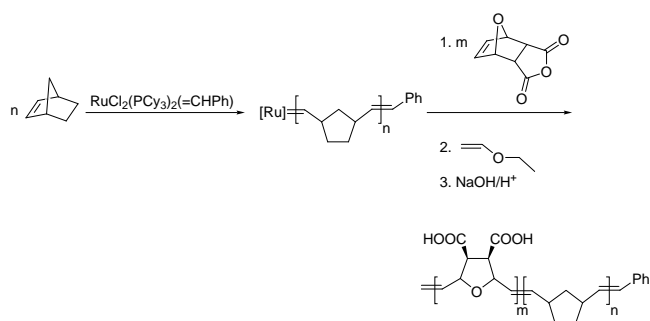[b] Below limit of quantification according to DIN 32645 [78].

for two reasons. On the one hand, the supports prepared by ring-opening metathesis precipitation polymerization had a low degree of cross-linking and could therefore not withstand the high pressures used in HPLC. On the other hand, simple molecules such as maleic acid loose some of their special properties, e.g. the *cis* configuration of the two carboxylic acid groups in course of radical polymerization since the two carboxylic acid groups are preferably located in a *trans*-position along the polymer chain [43]. Another drawback of free radical polymerization was related to the fact that well-defined block-copolymers are generally difficult to prepare by this technique, their block-size is hard to control and the capacity of the resulting stationary phase is therefore rather based on empirical knowledge than on stoichiometry. The fact, that functional (co-) polymers may be prepared via ROMP and that these are generally well-defined in terms of molecular weight, polydispersity

and polymer back-bone prompted us to extend our investigations onto the synthesis of soluble functional polymers and block-copolymers and the preparation of coated stationary phases therefrom. Aiming on the above mentioned *vic, cis*-dicarboxylic acids, we used a designed functional monomer, 7-oxanorborn-2-ene-5,6-dicarboxylic anhydride, and performed its controlled, living polymerization as well as copolymerization with norborn-2-ene (NBE). These (co-) polymers were used for the synthesis of coated stationary phases. By variation of the blocksizes, synergistic effects of the hydrophilic, carboxylic acid-functionalized part and the hydrophobic poly(NBE) part on separations could be studied and the optimum copolymer composition for particular HPIC-separations was determined.

7-Oxanorborn-2-ene-5,6-dicarboxylic acid (ONDCA) was an interesting molecule for various reasons. If the anhydric form is polymerized by ROMP-techniques and the resulting poly(anhydride) hydrolyzed to the corresponding dicarboxylic acid, the resulting polymer backbone consists of a vinylene-spaced poly(tetrahydrofurane) (poly-THF) with each unit bearing two *vic, cis*-configured carboxylic acids. The oxygen in the resulting five-membered ring significantly enhances the hydrophilicity compared to the parent poly(norborn-2-ene-5,6-dicarboxylic acid). In contrast to NBE-derivatives, which are preferably polymerized with molybdenum-based initiators, poly(ONDCA) was best prepared with ruthenium-based initiators, e.g. $RuCl_2(PCy_3)_2(CHC_6H_5)$. In case polymerizations were started with NBE, well-defined block-copolymers with regard to block-size and molecular weight, one block consisting of poly(ONDCA) and another of poly(NBE), could be prepared (Scheme 3). Table 8 gives an overview over these homo- and copolymers. Coated silica materials could be prepared in a reproducible way since the amount of polymer and consequently the carboxylate capacity (expressed in mmol/g) of the material was again simply determined by weight. Silica was dried and reacted with vinyltrimethoxysilane in order to obtain polymerizable groups at the surface and to convert as many surface silanol groups as possible
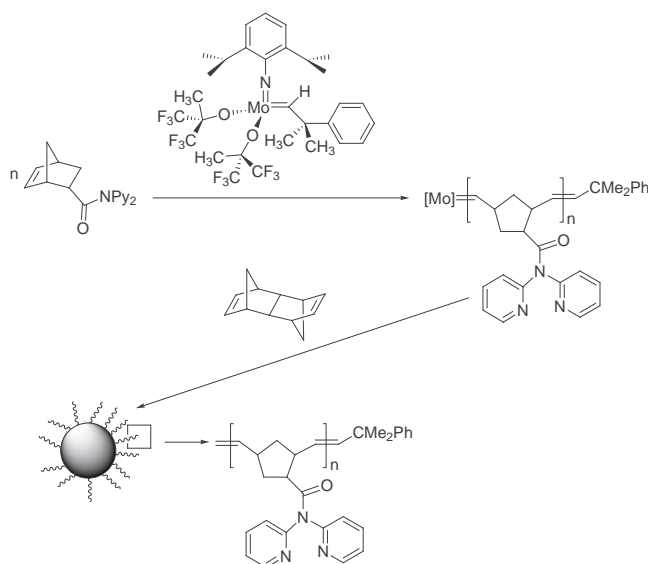
Scheme 2. Synthesis of dipyrid-2-yl-derivatized polymers via ring-opening metathesis precipitation polymerization.

Scheme 3. Synthesis and structure of block-copolymers used for the coating of silica.
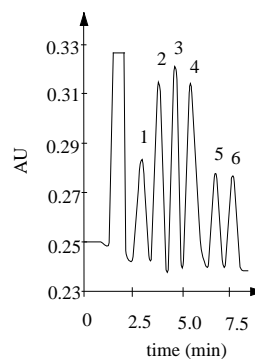

Fig. 1. Separation of 2,6-dimethylaniline (1), *N*-methylaniline (2), pyridine (3), *N,N*-dimethylaniline (4), 2,6-lutidine (5) and 3,4-lutidine (6) on Polygosil 60–10 coated with a poly(NBE$_{600}$-*b*-ONDCA$_{500}$) copolymer. Mobile phase: water/acetonitrile 98:2, 10 mm acetic acid, 7 mm triethylamine; flow rate: 1.0 mL/min; injection volume 5 μL (20 ppm each); detection: UV (254 nm).

Table 8
Properties of homo- and copolymers

	Material	M_w	PDI
A[a]	NBE$_{600}$-block-ONDCA$_{500}$	140.000	1.13
B[a]	NBE$_{600}$-block-ONDCA$_{200}$	88.000	1.31
C[b]	poly(NBE)$_{970}$	91.000	1.21
D[a]	poly(ONDCA)$_{770}$	130.000	1.22
E[a]	NBE$_{330}$-block-ONDCA$_{170}$	60.000	1.48

[a] Initiator RuCl$_2$(PCy$_3$)$_2$(CHPh).
[b] Initiator RuCl$_2$(PPh$_3$)$_2$(CHPh).

to silyl ethers. The exact amount of vinyl groups was determined by titration methods. Different amounts of prepolymer were deposited at the surface and finally cross-linked using thermal initiation (Table 9). The general quality of the coating method was checked by applying the standard Engelhardt test to a poly(NBE)-coated material [44]. No polar interactions of the analytes with the stationary phase, indicating the absence of any free silanol groups, were detected.

In order to obtain stable and efficient materials, different amounts of polymer (10–120 mg/g) were deposited onto the surface of various silica materials, resulting in polymer layers of various thickness (Table 9). Due to the high average molecular weights of the polymers, a loss of pore volume and specific surface area was observed particularly in the

case of materials with smaller pores compared to those with larger pore diameters. Thus, the specific surface area (σ) of silica with 60 Å pore diameter was reduced by a factor of two while 100 Å or 300 Å materials showed only a loss in σ of approximately 20%. The optimum coating thickness with regard to accessibility of the carboxylic acid groups was estimated by titration of the different materials. The amount of coating, expressed in μg polymer/m^2, was found to be a suitable measure. Thus, polymer coatings in the range of 50–120 μg/m^2 were found to be thin enough to allow an almost quantitative interaction (80–100%) of the carboxylic acid groups with the mobile phase without diminishing the chemical stability of the support.

3.1. Applications in HPLC

A typical separation achieved with these supports is shown in Fig. 1. High selectivities were achieved, as demonstrated by the fast (<8 min) baseline separation of six isomeric anilines and lutidines, which were similar with regard to pK_a

Table 9
Summary of coated materials

Polymer	Material[a]	V_p (mL/g)	d_{pore} (Å)	σ_1[b] (m^2/g)	σ_2[b] (m^2/g)	Coating (μg/m^2)	d[c] (nm)	H$^+$ (mequiv.) theoretical/found
A	Polygosil 60-10	0.75	60	450	180	260	0.23	0.77/0.21
A	LiChrosorb Si 60-7	0.75	60	500	250	240	0.21	0.77/0.25
A	LiChrosorb Si 60-7	0.75	60	500	270	50	0.03	0.16/0.13
A	LiChrosorb Si 60-7	0.75	60	500	287	180	0.12	0.6/0.49
B	LiChrosorb Si 60-7	0.75	60	500	244	230	0.13	0.42/0.39
C	LiChrosorb Si 60-7	0.75	60	500	160	240	0.23	0.00/–
A	Polygosil 100-7	1.0	100	300	233	380	0.27	0.74/0.38
A	Polygosil 300-7	0.8	300	100	79	1170	0.75	0.76/0.09
A	Nucleosil 50-7	0.8	50	450	274	240	0.21	0.69/0.56
D	Nucleosil 50-7	0.8	50	450	232	220	0.17	1.3/0.93
E	Silica 60	0.7–0.8	60	490	288	120	0.15	0.3/0.3

R: %C of coated material; T: carbon content of polymers A–E; ρ: polymer density ($\equiv$ 1 g/mL for simplicity).

[a] Silanized with vinyltrimethoxysilane.
[b] Specific surface area prior (σ_1) and after (σ_2) coating.
[c] d: thickness of polymer layer, calculated from $S = (R/T) \times 1000/(1 - (R/T)\sigma_1\rho)$ [79].

values, size and chemical properties. Separation efficiency was positively influenced by the presence of the non polar sites from the poly(NBE) block. The importance of such sites suggests some additional reversed-phase interaction of the analytes with the material, the more, since separation of these analytes on a poly(ONDCA) homopolymer-based column was poor. The use of various block sizes in the copolymers revealed no significant change in selectivity. Roughly, a 1:1 ratio of NBE and ONDCA was found suitable.

Furthermore, the successful separation of isomeric hydroxyquinolines [39] as well as of various flavones [45] need to be mentioned. Particularly for the latter, the new stationary phases allowed fast separations even at extreme pH values. For further characterization, a LC system was coupled to a quadrupole ion trap mass-spectrometer via an electrospray ionization interface (ESI). Finally, using a poly(NBE$_{600}$-*b*-ONDCA$_{500}$)-coated Nucleosil 50-7 in combination with this LC–ESI-MS/MS setup, the fast characterization and quantification of flavonoids present in onions, elderflower-blossom, lime-blossom, St. John's Wort and red wine was made possible.

3.2. On-line SPE-RP-ion-pair HPLC of lanthanides [22,30,46,47]

Encouraged by the good extraction capabilities of carboxylic acid derivatized, ring-opening metathesis precipitation polymerization-derived SPE supports, we investigated whether the new coated supports could again be used for the enrichment of lanthanides. The main objective was to overcome the restrictions both in terms of narrow extraction pH and pressure instability given by the above-described ring-opening metathesis polymerization-derived SPE support. Particularly, a method for the fast on-line routine analysis of REEs was to be developed. A ROMP-derived block-copolymer, poly(NBE$_{600}$-*b*-ONDCA$_{500}$), was used for coating purposes. As in previous studies [22,30], a GSR-3 basalt and GSR-1 andesite were used as certified materials. In a first step, polymer coated silica 60 [39] was used for the extraction of two radioactive lanthanides, ^{152}Eu, and ^{147}Pm [47]. The coated silica showed high extraction efficiencies for these two lanthanides as determined by standard SPE experiments using β-liquid scintillation counting for quantification. Extraction efficiencies, determined over a concentration range of 23 ng/l–250 mg/l, thus covering a range of 7 orders of magnitude, were quantitative in all cases. A first important finding was that the pH for lanthanide extraction could be extended to a range of 3.5–5.5. This significantly improved complexation of REEs by the new ligand was attributed to the presence of the additional ether-functionality in each five-membered ring, resulting from the ROMP of ONDCA, which was not present in the poly(norborn-2-ene-5,6-dicarboxylic acid-*co*-1,4,4a,5,8,8a-hexahydro-1,4,5,8-*exo-endo*-dimethanonaphthalene) system [30]. Recovery, HPLC as well as ICP-OES experiments confirmed the high selectivity of the

new sorbent for lanthanides. These investigations revealed that the retention of potentially interfering metal ions such as Mg^{2+}, Ca^{2+}, Ba^{2+}, Mn^{2+}, Co^{2+}, Ni^{2+}, Al^{3+}, Fe^{3+}, Zn^{2+} by the new sorbent was less than 5% in all cases. Encouraged by these findings, we designed an on-line SPE-HPLC system as shown in Fig. 2. Precolumns of different sizes were packed with poly(NBE$_{600}$-*b*-ONDCA$_{500}$) coated Silica-60. Separation of REEs was accomplished using RP-ion-pair chromatography. For these purposes, a gradient separation system consisting of hydroxyisobutyric acid (HIBA) and sodium octadecylsulfonate was found suitable. As in previous studies, rock digests were again modified with 5-sulfosalicylic acid in order to mask Fe^{3+} and Al^{3+} [30]. Since especially granites possess a high Si-content and *ortho*-silicic acid shows a minimum in solubility around pH 5, methanol was again added to prevent the formation of polysilicic acid. The entire solution was adjusted to a pH of 4.0 and passed over coated Silica-60-packed precolumns (60 mm × 4 mm). REE concentrations prior to enrichment were typically in the range of 1–25 ng/mL, the total amount of each REE sorbed onto the pre-column was in the range of 8–270 ng. Recoveries were calculated on the basis of REE chromatograms obtained from direct injection of the corresponding REEs using either 4-(2-pyridylazo)resorcinol (PAR) or arsenazo III as post-derivatization reagents. As can be deduced from Table 10, quantitative recoveries (97–103%) were obtained for most REEs. Except for Pr, Dy + Y and Ho, R.S.D.s were within a range of 2–5%.

3.3. SPE of noble metals

In order to obtain an SPE support capable of the extraction transition metal ions, a 4′-(norborn-2-en-5-ylmethylenoxy)terpyridine was copolymerized with NBE *via* Mo(*N*-2,6-*i*-Pr$_2$-C$_6$H$_3$)(CHCMe$_2$Ph)(OC(CH$_3$)(CF$_3$)$_2$)$_2$-catalyzed ROMP to give a poly(NBE$_{900}$-*b*-4′-(norborn-2-en-5-ylmethylenoxy)terpyridine$_{60}$) block-copolymer (Fig. 3). This block-copolymer was used for the preparation of
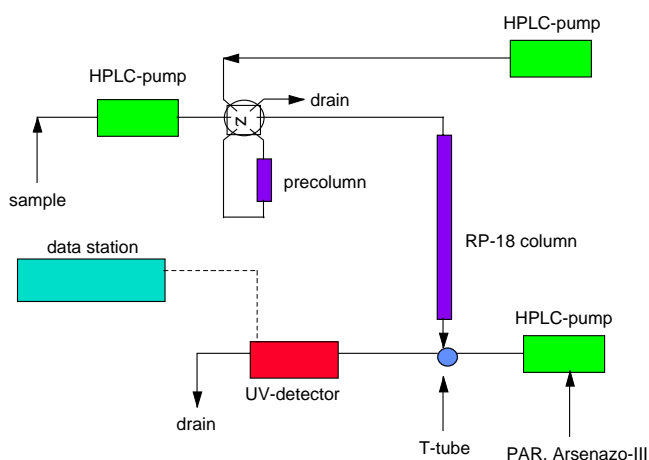

Fig. 2. Schematic drawing of the on-line SPE-RP-ion-pair-HPLC system.

Table 10
Recoveries (%) and σ_{n-1} for La–Lu (without Pm) after enrichment on coated silica-60

Sample		La	Ce	Pr	Nd	Sm	Eu	Gd	Tb	Dy + Y	Ho	Er	Tm	Yb	Lu
Standard[a]	Concentration (ng/mL)	50	50	50	50	50	50	50	50	50	50	50	50	50	50
	Recovery (%)	100	98	101	97	101	102	97	99	98	101	102	103	103	100
GSR-3[b]	Concentration (ng/mL)	14.0	26.3	6.6	13.5	15.3	4.8	4.3	6.0	6.9	4.4	1.0	–	0.75	–
	Recovery (%)	104	103	100	103	99	94	103	98	103	94	98	c	95	c
	σ_{n-1}	2	2	7	4[b]	4	0	4[b]	2	3	1	3	–	2	–
GSR-1[d]	Concentration (ng/mL)	13.5	27.0	19.1	11.8	14.6	4.3	14.0	8.3	18.1	1.0	3.3	5.3	3.7	5.8
	Recovery (%)	99	100	99	103	97	98	100	97	100	112	99	106	103	99
	σ_{n-1}	4	0	7	6	5	2	5	4[b]	6	7	3	4	5	5

pH 4.
[a] $n = 3$.
[b] $n = 5$.
[c] Below limit of quantification according to DIN 32645.
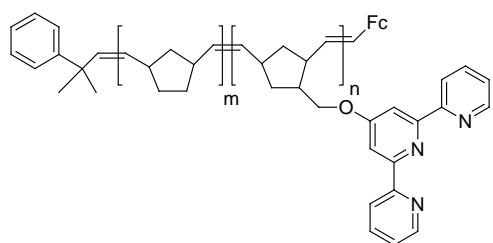[d] $n = 3$.

Fig. 3. Structure of poly(NBE$_{900}$-*b*-4′-(norborn-2-en-5-ylmethylenoxy)-terpyridine$_{60}$).

polymer-coated silica-60 (4.8 wt.% coating). While no main group elements were extracted by this supports, the selectivity order under competitive conditions at pH < 0.6 was Pd ≈ Ag ≈ Au ≈ Pt > Re > Ir > Rh > Ru > Fe > Cr ≈ Mn ≈ Cd ≈ Zn. Enhanced selectivity was observed at pH 3.5, here the extraction order was Au > Hg > Pd ≈ Ag > Rh > Pt > Ir ≈ Re > Cu > Co ≈ Zn ≈ Cd ≈ Ni > Cr > Mn. Even under competitive conditions, loadings of >6 mg/g were realized for Au(III) and Hg(II). Quantitative recoveries >97% were observed for all metal ions [48].

4. Surface-grafted supports prepared via metathesis polymerization [49]

The surface-grafting of polymers represents a well-established and useful procedure for the preparation of certain polymer architectures. So far, surface grafting was mainly based on free radical polymerization techniques using styrene and various acrylates, respectively [50]. To obtain materials suitable for applications in HPLC and to avoid the loss of surface area related to pore clogging phenomena observed with coating procedures, we focused on the development of ROMP-based grafting techniques applicable to the preparation of new graft-type supports. In order to gain access to supports suitable for chiral separations, various chiral monomers were chosen for the preparation of surface-grafted supports on the base of their polymerization characteristics

with metal initiators. They are summarized in Fig. 4. Using both Grubbs- (RuCl$_2$(PCy$_3$)$_2$(CHPh)) and Schrock-type (Mo(*N*-2,6-Me$_2$-C$_6$H$_3$)(CHCMe$_2$Ph)(OCMe(CF$_3$)$_2$)$_2$) initiators, silica as well as PS-DVB-based supports were successfully grafted with these monomers. Copolymerizable anchoring groups were used for the attachment (grafting) of the actual working functionalities. Here, the extent of derivatization was dependent on both the amount of anchoring groups and the amount of monomer used. Generally speaking, the simplest way of providing suitable anchoring groups for the preparation of a ROMP-graft-copolymer was the surface-attachment of norborn-2-ene-5-yl-groups. This was easily accomplished in the case of silica materials using trichloro-norborn-2-ene-5-ylsilane. Subsequent "endcapping" with a mixture of chlorotrimethylsilane and dichlorodimethylsilane lead to a sufficient derivatization of the remaining surface silanol groups. In the case of PS-DVB-based materials, bromomethylations using trioxane, tin tetrabromide and trimethylbromosilane were performed [51]. Alternatively, conversion of the chloromethyl groups into to the more reactive bromomethyl groups was accomplished via halogen exchange [52]. Finally, the bromomethylated PS-DVB resins were converted into the norborn-2-ene-5-ylmethylethers. For grafting, both a "grafting-from" as well as a "grafting-to" approach could be realized. Particularly, the latter required at least a class-IV living system [3] and consequently lead to the formation of tentacle-type stationary phases with the linear polymer chains pointing away from the support. The amount of graft polymer was in the range of 0.04–2 mmol/g. Measurements of the specific surface areas (σ) prior and after grafting using N$_2$-adsorption revealed that changes in σ were less than 10% in course of the grafting procedure. This was true for both non-porous PS-DVB- and porous silica-based materials, indicating that the pores were not filled with graft-polymer. In terms of materials chemistry it is worth noting that silica prepared via a "grafting-from" approach exhibited an enhanced stability compared to standard surface-modified silica and could be used within a pH range of 2–10. In order to perform a direct comparison between coated and grafted
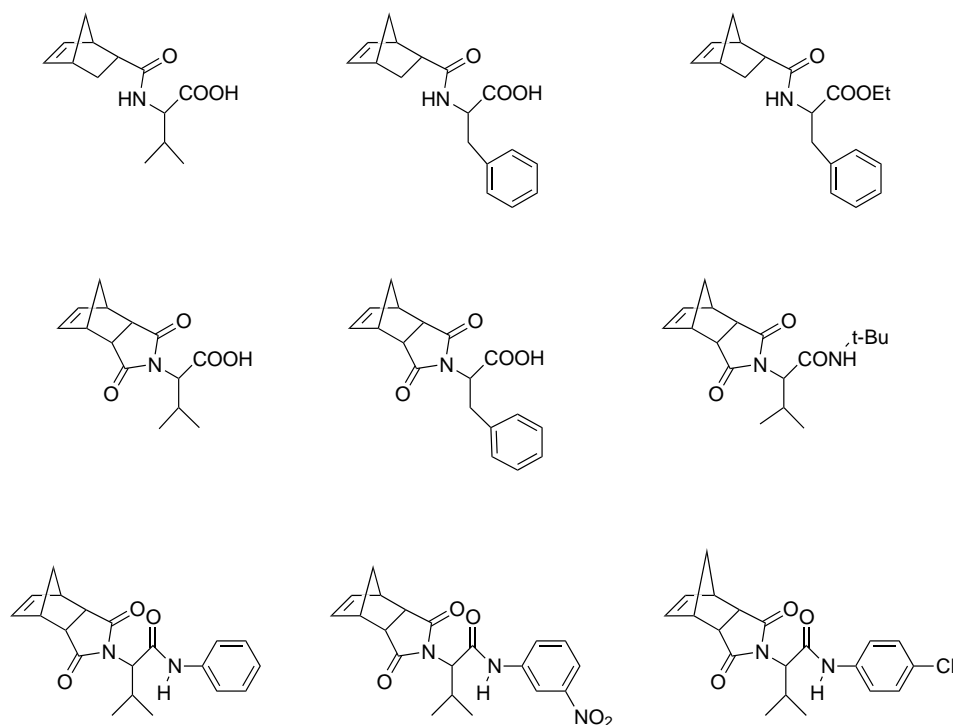
Fig. 4. Structure of chiral monomers used for surface grafting.

stationary phases, a series of poly(ONDCA), as well as poly(NBE-co-ONDCA) based silica supports were prepared via ROMP using both coating and grafting techniques. In a preliminary experiment, the new stationary phases were used for the separation of a series of anilines and lutidines [53]. As expected, grafted supports possessed superior separation capabilities compared to their coated analogues. Similar to coated stationary phases, supports prepared by the subsequent grafting of NBE and ONDCA yielded poly(NBE-co-ONDCA) graft-copolymers, which possessed both hydrophobic and ion-exchange sites and represented optimum stationary phases particularly for the separation of isomeric basic analytes. Thus, poly(NBE-co-ONDCA) grafted ion exchange supports showed the highest number of theoretical plates (up to 16,000) in the separation of 2,6-dimethylanilinen, *N*-methylaniline, pyridine, *N,N*-dimethylaniline, 2,6-lutidine, and 3,4-lutidine compared to the homopolymer-grafted supports poly(NBE) silica and poly(ONDCA) silica as well as to block-copolymer coated silica. Similar results were observed in the separation of 4 isomeric hydroxyquinolines.

4.1. Synthesis of chiral stationary phases (CSPs) [54–56]

Chiral chromatography is an important, if not the most important tool for analytical and preparative scale separations of enantiomers. While various routes for the enantioselective synthesis of chemical compounds, drugs and pharmaceuticals have been developed, a major part of chiral compounds is still produced as a racemate and needs to be separated into both enantiomers by chiral HPLC prior to

use. Despite the large variety of systems that are available so far, intense research still focuses on the economical development of more stable, more efficient and more selective chiral separation systems. Using the new ROMP-derived CSPs, baseline separation ($\alpha = 2.0$, $R_s = 1.91$) of dinitrobenzoylphenylalanine was achieved on poly(*N*-(norborn-5-ene-2-carboxyl)-L-phenylalanine ethylester)-grafted Nucleosil 300-5 [54]. Alternatively, various NBE-derivatized β-cyclodextrins (β-CDs) were synthesized and surface grafted onto silica-based supports using ROMP. The resulting CSPs were be prepared with high reproducibility and used for the enantioselective separation of β-blockers, *N*-dansyl-, *N*-3,5-dinitrobenzoyl- and Fmoc-protected amino acids [55]. Excellent results were obtained in terms of chemical stability, selectivity (α') and resolution (R_s). For the above-mentioned analytes, values for α' and R_s up to 3.40 and 7.67, respectively, were obtained. Furthermore, the new CSPs were investigated for their separation capabilities for a series of the planar chiral ferrocene derivatives, e.g. *rac*-ferroceno[2,3*a*]inden-1-one, *rac*-6-(3-hydroxy-3-methylbut-1-yn-1-yl)ferroceno[2,3*a*]inden-1-one [56]. These compounds were again successfully separated, here values for α' and R_s of 2.15 and 2.70, respectively, were obtained. A typical separation shown in Fig. 5.

4.2. Supports for anion-exchange chromatography of oligonucleotides [57]

Oligonucleotides synthesized by standard solid-phase synthesis are usually contaminated with failure sequences
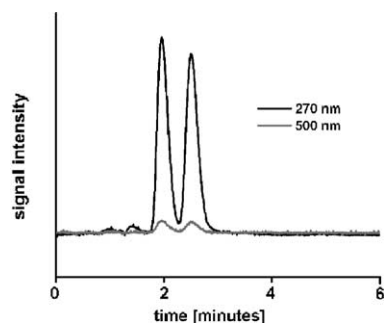
Fig. 5. Separation of *rac*-ferroceno[2,3*a*]inden-1-ones on a poly-(tetrakis(*endo/exo* -6- *O*- norborn-2- ene-5- ylmethoxymethylsilyl)- β- CD)-grafted column. Conditions: $T = 21.5\,^{\circ}C$; flow, 0.5 mL/min; acetonitrile–MeOH–acetic acid–triethylamine, 90:10:0.15:0.45; detection, UV.

and partially deprotected sequences, respectively. Therefore, purification and careful quality control are mandatory. In this context, we investigated the use of poly(ferricinium)-grafted mesoporous silica prepared by a "grafting-to approach" in anion exchange chromatography of oligonucleotides. For this purpose, three different ethynyl-substituted ferrocenes and octamethylferrocenes, respectively, were grafted to mesoporous and non-porous silica (Nucleosil 300-5 and Micra, respectively) via alkyne metathesis polymerization using $Mo(N\text{-}2,6\text{-}Me_2\text{-}C_6H_3)(CHCMe_2Ph)(OCMe(CF_3)_2)_2$ (Scheme 4). Typical amounts of grafted monomer were in the range of 5–50 μmol/g. Since ferrocene and particularly octamethylferrocenes are easily oxidized, the resulting poly(ferrocene)-grafted supports were treated with a solution of iodine in acetonitrile to yield the corresponding poly(ferricinium)-based stationary phases.

With these anion exchange supports in hand, particularly non-porous grafted Micra was successfully used for the separation of synthetic homologous oligodeoxythymidylic acids $(dT)_{12-18}$. Separation was accomplished within less than 7 min, peak widths at half height were between 0.15 and 0.20 min. It is worth noting that the separation

performance achieved with such non-porous octamethyl-ferricinium material came very close to that described for the separation of $(dT)_{12-18}$ on poly(ethylenimine)-coated non-porous silica (PEI-silica) [58] or on commercial, non-porous diethylaminoethyl-polymer-based stationary phases [58].

5. Monolithic ROMP-derived supports [59,60]

5.1. Synthesis and properties

Monolithic separation media evolved as a successful "joint-venture" between material and separation sciences. Based on theoretical reflections, the common idea was to produce a support with a high degree of continuity that should meet the requirements for fast, yet highly efficient separations [61,62]. Generally speaking, the term "monolith" applies to any single-body structure containing interconnected repeating cells or channels. Such supports are either prepared from inorganic mixtures, e.g. silanols, or from organic compounds, e.g. by a cross-linking polymerization. Here, the term "monolith" or "rigid rod" shall comprise cross-linked, organic materials which are characterized by a defined porosity and which support interactions/reactions between this solid and the surrounding liquid phase. Besides advantages such as lower back pressure and enhanced mass transfer [63,64], the comparable ease of fabrication as well as the many possibilities in structural alteration have to be mentioned. Due to the broad applicability of ROMP and the good definition of the resulting materials, this transition-metal catalyzed polymerization was used for the synthesis of monolithic polymers [65]. We found that this may be accomplished by generating a continuous matrix by ring-opening metathesis copolymerization of suitable monomers with a cross-linker in the presence of porogenic solvents within a device (column). For sake of
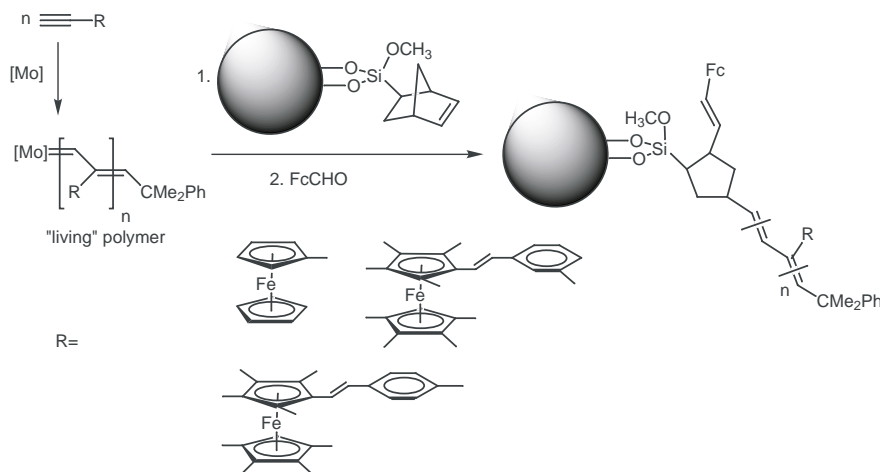
Scheme 4. Surface grafting via alkyne metathesis polymerization. Fc = ferrocenyl.

clarity, some important synthetic features relevant for the synthesis of ROMP-derived monolithic supports, need to be summarized.

The choice of a suitable initiator represents a crucial step in creating a well-defined polymerization system in terms of initiation efficiency and control over propagation. Only in the case where a quantitative and fast initiation occurs, the entire system may be designed on a *stoichiometric base*. This is important, since for control of microstructure, the composition of the entire polymerization mixture needs to be varied within extremely small increments. Generally, a ruthenium-based Grubbs-type initiator, $(RuCl_2(PCy_3)_2(=CHPh)$, Cy = cyclohexyl) was used. Among the possible combinations of monomers and cross-linkers the copolymerization of NBE with DMN-H_6 in the presence of two porogenic solvents, 2-propanol and toluene, with $RuCl_2(PCy_3)_2(=CHPh)$ was found to work best (Scheme 5). In terms of construction, monoliths consist of microstructure-forming microglobules, which are characterized by a certain diameter (d_p) and microporosity (ε_p). Sum of volume fractions of both micropores and voids (intermicroglobule porosity) is the total porosity (ε_t). This value represents a percentage of pores in the monolith and can together with the pore size distribution, the total pore volume (V_p), and the specific surface area (σ) be calculated from inverse size exclusion chromatography (ISEC) data [25]. Although somewhat controversial [66,67], this method presents a suitable way to perform such measurements as it operates under conditions similar to those used in actual HPLC separations. Furthermore, the choice of PS-standards allows the determination of the specific surface area and porosity relevant for chromatographic separations [53]. In order to design monolithic supports for different separation tasks, we developed a method that allowed the variation of relevant structural parameters in a controlled and reproducible way. In this context, each component of the polymerization mixture, i.e. NBE, DMN-H_6, solvents, and initiator as well as temperature were variables that were used to a certain extent for this purpose [65,68]. The influence of every singly component was studied extensively, nevertheless, a detailed description has to be omitted for obvious reasons. Table 11 summarizes some of the structural variations that can be achieved. As shown, the volume fraction of the interglobular void volume (ε_z) and ε_t may be varied within a range of 0–50 and 50–80%, respectively.

Monoliths prepared by ROMP were evaluated by measurement of the pressure drop across the column using different solvents and a wide range of flow rates. The linearity of plot confirmed that the monoliths were not compressed even at high flow velocities exceeding 5 mm/s. When dealing with transition metal catalyzed polymerizations, the efficiency of metal removal from the monolith after polymerization needs to be addressed. The fact that ruthenium-initiated polymerizations may conveniently be capped with ethyl vinyl ether was demonstrated by ICP-OES investigations on the Ru-content of the final rods. These investigations revealed Ru concentrations $<10\,\mu g/g$, corresponding to a metal removal $>99.8\%$.

5.2. Applications in the separation of biomolecules

Nonpolar, non-functionalized polymeric surfaces are widely used as stationary phases for both RP-HPLC and IP-RP-HPLC. While the former is the method of choice for high-resolution separations of peptides and proteins, the latter is eminently suited for the separation of single- and
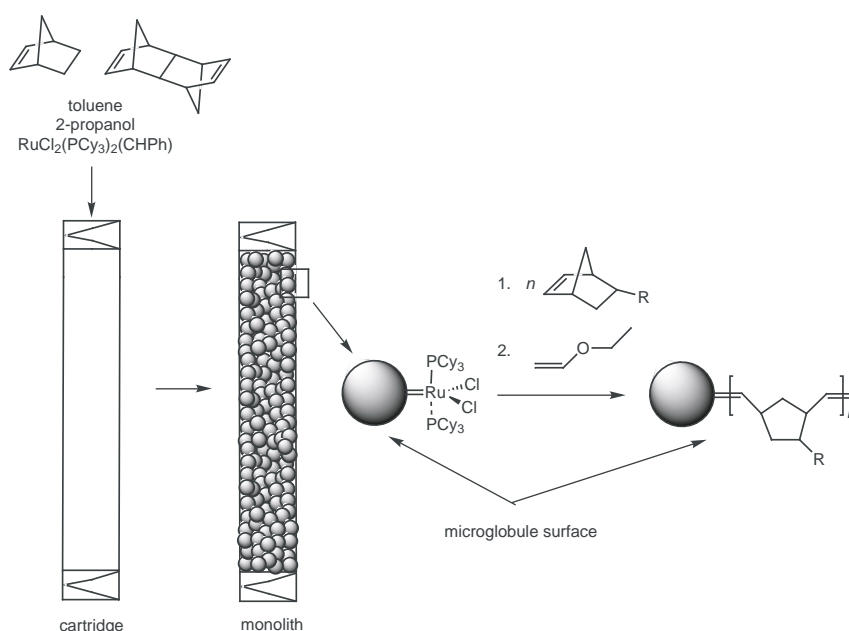
Scheme 5. Synthesis and functionalization of ROMP-derived monolithic supports.

Table 11
Physico-chemical data of ROMP-derived monoliths

NBE (%)[a]	DMN-H$_6$ (%)[a]	Toluene (%)[a]	2-PrOH (%)[a]	Cat (%)[a]	T_p (°C)	σ (m^2/g)	ε_p (%)	ε_z (%)	ε_t (%)	V_p (mL)	d_p (μm)
15	15	10	60	0.4	0	76	43	37	80	0.31	2 ± 1
20	20	10	50	0.4	0	62	43	33	76	0.31	4 ± 1
25	25	10	40	0.4	0	85	48	15	63	0.34	2 ± 1
25	25	10	40	1	0	86	48	14	63	0.34	4 ± 1
30	30	10	30	0.4	0	191	50	5	54	0.35	8 ± 2
30	30	10	30	1	0	96	50	2	53	0.36	6 ± 2
15	15	20	50	0.4	0	110	39	49	89	0.28	3 ± 1
20	20	20	40	0.4	0	74	44	21	65	0.31	4 ± 1
25	25	20	30	0.4	0	91	47	15	62	0.33	4 ± 1
30	30	20	20	0.4	0	93	65	5	69	0.46	4 ± 1
0	50	10	40	0.4	0	88	44	25	69	0.31	2 ± 1
15	35	10	40	0.4	0	76	45	26	71	0.32	4 ± 1
25	25	10	40	0.4	0	85	48	15	63	0.34	2 ± 1
35	15	10	40	0.4	0	100	45	10	56	0.32	3 ± 1
25	25	10	40	0.1	0	83	49	20	69	0.35	2 ± 1
25	25	10	40	0.4	0	85	48	15	63	0.34	2 ± 1
25	25	10	40	1	0	75	49	12	61	0.35	3 ± 1
25	25	10	40	0.4	−30	97	50	13	63	0.35	8 ± 2
25	25	10	40	0.4	−20	98	45	17	62	0.32	6 ± 2
25	25	10	40	0.4	−10	85	47	10	58	0.33	4 ± 2
25	25	10	40	0.4	0	85	48	14	63	0.34	2 ± 1

T_p: polymerization temperature; d_p: microglobule diameter.

[a] By weight.

double-stranded nucleic acids. Using ROMP-derived monoliths, the separation of oligothymidylic acids (dT)$_{12-18}$ ranging in mass from 3638 Da (dT$_{12}$) to 5456 Da (dT$_{18}$) was accomplished on a semipreparative scale in 2 min (Fig. 6) [69]. As expected, the elution order of oligodeoxynucleotides strongly correlated with their molecular mass since increasing molecular mass directly translates into an increase in hydrophobic interaction of the corresponding analyte with the rod. In addition, a mixture of eight proteins (ribonuclease A, insulin, cytochrome c, lysozyme, α-lactalbumin, α-chymotrypsinogen A, β-lactoglobulin B, catalase) was separated in less than 50 s by RP-chromatography [69].

Encouraged by the high efficiency of these columns, we turned our attention to the separation of double-stranded (ds)
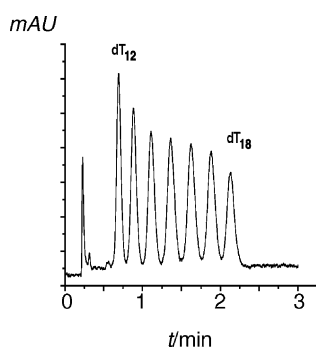

Fig. 6. IP-RP-HPLC separation of a oligodeoxynucleotides (dT)$_{12-18}$ on a ROMP-derived monolith (3 mm × 60 mm). Mobile phase: 100 mmol/l triethylammonium acetate at pH 7.0; linear gradient: 11–16% acetonitrile in 10 min; flow rate: 2 mL/min; T = 20 °C; detection: UV (264 nm); sample: (dT)$_{12-18}$, 0.1 μg of each oligodeoxynucleotide.

DNA [70]. The separation and fraction of dsDNA fragments is a key element in various molecular biological experiments, including cloning, DNA sequencing, genome fingerprinting, DNA hybridization, and mutation detection. The mixture of fragments generated by the enzymatic cleavage of DNA with restriction endonucleases may range from a few base pairs to thousands of base pairs, depending on DNA size, DNA sequence and the restriction enzyme used. The separation of pBR322 DNA-*Hae*III fragments required both a careful tuning of the monolithic structure and the addition of a modifier. Based on a report describing the influence of glycerol on dsDNA separations by capillary electrophoresis, [71] we investigated as to which extent this method was applicable to HPLC separations of dsDNA on monolithic systems. A separation using a two-step gradient using 4% (v/v) glycerol is shown in Fig. 7. The amount of DNA material that could be loaded onto a 100 mm × 3 mm i.d. column without serious loss in separation efficiency was about 2.5 μg. Although this amount suffices for most experiments involving nucleic acids, the process can be readily upscaled by using monolithic columns of larger dimensions.

5.3. Miniaturized systems: monolithic capillary columns [72]

In order to contribute to ongoing efforts towards the miniaturization of analytical devices and to develop systems applicable to the coupling to highly sensitive quantification methods such as mass spectroscopy (MS), we investigated whether the concept of ROMP-derived monolithic supports could be extended to the synthesis of capillary columns.
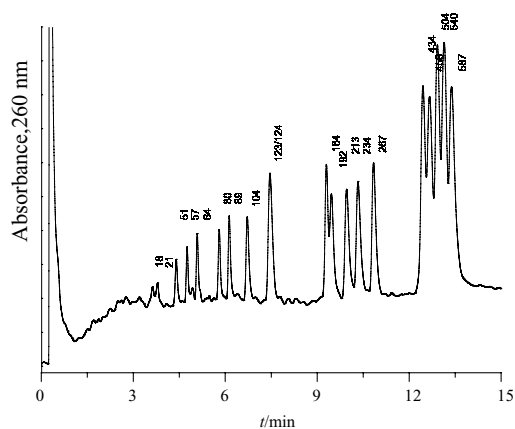
Fig. 7. Influence of glycerol as a mobile phase additive in the separation of dsDNA fragments. Mobile phase: A, 0.1 mol/l triethylammonium acetate, pH 7.0, 4% glycerol; B, 0.1 mol/l triethylammonium acetate, pH 7.0, 40% acetonitrile, 4% glycerol; gradient, 10–25% B in 5 min, 25–45% B in 12 min; flow rate, 2.0 mL/min; temperature, 50 °C; sample, 0.75 μg pBR322 DNA-*Hae*III digest.

A separation of single-stranded oligodeoxynucleotides by IP-RP-HPLC on a monolithic ROMP-derived capillary column is illustrated in Fig. 8. Using 0.2 mm i.d. capillaries, high resolution was achieved for all six analytes ($2.27 < R_s < 3.47$). In addition, four homologous oligodeoxynucleotides, ranging in length from 24–27 nucleotides and differing from each other by the insertion of one, two and three thymidines after position 18 of the 24-mer were baseline separated within 7 min [72].

Fig. 9 depicts the analysis of a mixture of dsDNA fragments obtained by digestion of the pBR322 plasmid with the restriction enzyme *Hae*III. The fragments ranging in size from 51 to 587 base pairs were separated by capillary IP-RP-HPLC. The excellent separation efficiency of ROMP-based monoliths for dsDNA was documented in peak width at half height of 3.1–8.5 s for the fragments up to about 250 base pairs. Longer DNA fragments eluted with peak widths at half height around 10–12 s due to the shallower gradient required for total resolution. This
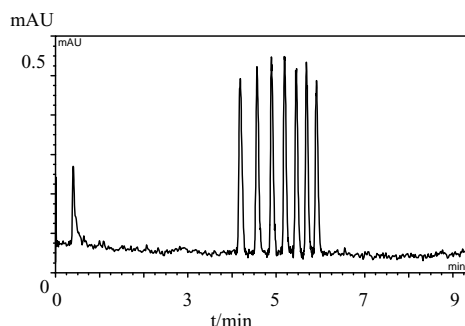

Fig. 9. Separation of dsDNA on a monolith ($0.2 \, mm \times 60 \, mm$): mobile phase, 4–10% acetonitrile in 1 min, 10–16% ACN in 14 min in 0.1 M $Et_3NH^+OAc^-$ (pH 7.0), 1% MeOH; flow, 3 μL/min.

separation is another example for the improved separation performance of ROMP-based capillary monoliths compared to their analogues in the analytical 3-mm format. While the separation of the 184/192 base pair fragments was incomplete on the 3 mm i.d. monolith [70] the two fragments were almost separated to baseline in the 200 μm capillary monolith.

Finally, the hydrophobic stationary phase was tested for the separation of some proteins by RP-HPLC. Fig. 10 illustrates the separation of six proteins (ribonuclease A, insulin, cytochrome c, lysozyme, α-chymotrypsinogen A, catalase) by capillary RP-HPLC at a flow rate of 6 μL/min. The use of a steep gradient ensured the rapid elution of the proteins as extremely sharp peaks with peak widths at half height of 1–2 s. The selectivity was high, allowing the separation of all components to baseline within less than 5 min and still leaving left space for additional peak capacity. Finally, it is worth mentioning that these supports are also capable of separation diastereomeric phosphorothioates [72].

Fig. 8. Separation of (pdT)$_{12-18}$ (10 ng) on a monolith ($0.2 \, mm \times 100 \, mm$): mobile phase, 200 mmol/l triethylammonium acetate (pH 7.0); linear gradient, 8–16% acetonitrile in 10 min; flow, 5.3 μL/min; $T = 20 °C$; detection, UV (254 nm).
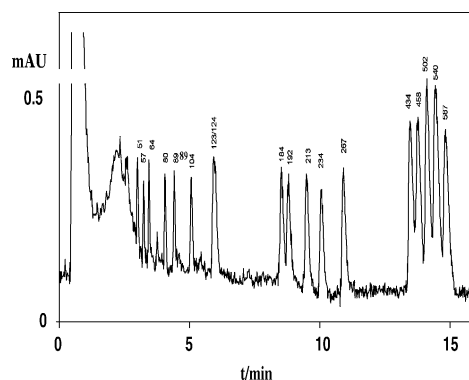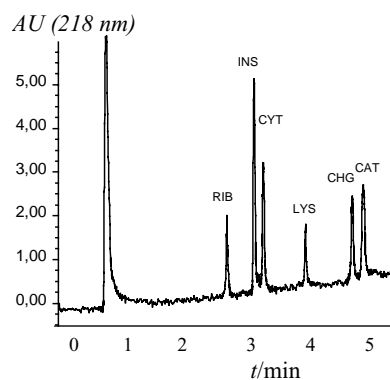

Fig. 10. Separation of proteins (ribonuclease, insulin, cytochrome c, lysozyme, α-chymotrypsinogen A, catalase) on a monolith ($0.2 \, mm \times 220 \, mm$). Mobile phase A: 0.05% aqueous TFA, B: ACN + 0.05% TFA; linear gradient: 10–100% B in 10 min; delay: 2 min; RT, flow: 5.71 μL/min (400 mL/min + 50/375/40 cm split); 180 bar; injection volume: 500 nl; concentration: 10 μg/mL.

5.4. Monolithic ROMP-derived columns for SEC [73]

High-throughput screening (HTS) has become a versatile tool in synthetic chemistry. While various approaches based on combinatorial chemistry have been developed for catalyst synthesis and even fast analytical tools are nowadays available for their characterization, the fast analysis of polymers prepared therefrom, usually accomplished by SEC, still represents a bottleneck. We were therefore interested in the synthesis of monolithic supports for fast non-aqueous SEC. This approach was characterized by some principle impediments based on the entirely different morphologies of monoliths used in HPLC and GPC. In contrast to monolithic HPLC supports, which allow fast separations because of the lack of micro and mesoporosity, monolithic supports suitable for GPC required a *continuous porosity*. Therefore, the major task was to develop a metathesis-based polymerization system that allows the in situ formation of the desired polymeric structure. In other words, a suitable ratio of micro-, meso- and macropores had to be formed simultaneously during rod formation. In addition, in order to be applicable to HTS, separation times had to be reduced to a minimum. Such monolithic GPC supports were realized using a mixture of *two* cross-linkers, DMN-H_6 and (NBE-$CH_2O)_3SiCH_3$, for monolith synthesis. On one hand, such a mix gave access to sufficiently cross-linked and thus long-term stable monoliths, one the other hand they possessed the favorable intermediate pore size distribution with about 50% of the pores in the micropore region below 12.5 Å resulting from the use of DMN-H_6. For column dimensions of 250 mm × 5 mm, the optimum flow rate was found to be 0.5 mL/min. To confirm reproducibility in elution, PS 17,600 was injected 30 times. Excellent stability in terms of retention time t_R was observed. Thus, the average value for t_R was 4.499±0.001 min, corresponding to a RSD of 0.031%. A third order calibration curve was recorded for standards in a range of 2600 to 3,280,000 Da (Fig. 11). A good fit for these narrow PS standards with $R^2 = 0.994$ was obtained. It should be emphasized, that monolithic columns described here were also used for the quantification of oligomers in the range of 72 to 1220 Da. For this purpose, a separate calibration curve
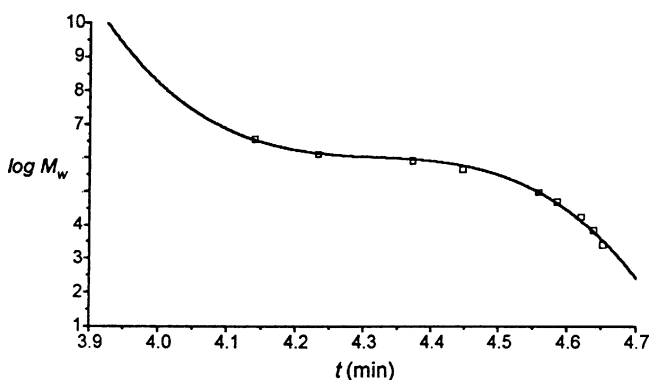
was recorded for this particular range. In order to check the quality of the new systems, nine different narrow PS standards ranging from 265–1,500,000 g/mol were applied for unknown quantification. Deviations in the calculated average molecular weight of these samples were significantly lower compared to a commercial column. Nevertheless, the most important feature of the new supports was the reduction in separation times to less than 5 min for molecular weights of 2000–1,300,000 Da. This allowed their use in high-throughput analysis of polymer samples, e.g. obtained from combinatorial polymerization catalyst screening.
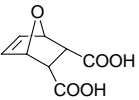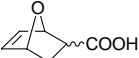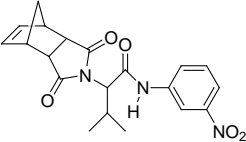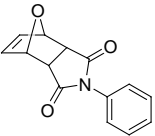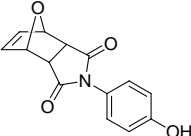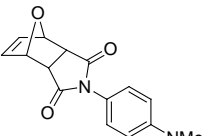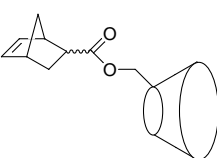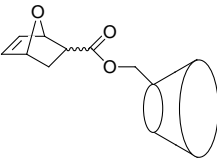
5.5. Functionalization

Grubbs-type initiator-based ROMP is usually a living polymerization process. Using the active initiator covalently bound to the surface of the structure-forming microglobules after completed rod-formation, various functional monomers were grafted onto the monolith surface by simply passing solutions thereof through the mold (Scheme 5). Tentacle-type polymer chains attached to the surface were formed. Generally speaking, this approach offered multiple advantages. First, the structure of the "parent" monolith was not affected by the functional monomer and could be optimized regardless of the functional monomer used later. Second, solvents other than the porogens toluene and methanol (e.g. methylene chloride, DMF) could be used for the "in situ" derivatization [74]. The versatility of this concept was demonstrated by the large variety of functional monomers shown in Table 12 that were grafted to the surface of monolith. For convenience, all monomers were based on norborn-2-ene or 7-oxanorborn-2-ene. Using a ß-CD-derivatized monolith, the chiral separation of proglumide was accomplished [65]. For purposes of completeness it should be noted that a post-synthesis grafting method recently developed in our group now offers access to high-capacity functionalized monolithic systems. Such high-capacity monoliths are very vital for various applications such as catalysis, extraction of environmental contaminants, extraction of biochemicals for either pharmaceutical or clinical purposes or, more general, separation techniques [75]. With these systems, the amounts of grafted monomers can exceed 1 mmol/g [76].

6. Summary

In summary, metathesis-based stationary phases described in this contribution add another dimension to the family of non-conventional separation media. They possess a non-aromatic polymer backbone and may be prepared in a reproducible way. An almost unlimited range of functional groups may be introduced, the degree of functionalization can be varied between 0 and approximately 8 mmol/g. Important enough, pressure stable systems, either silica- or monolith-based, are accessible. Both the large number of

Fig. 11. Calibration curve for a monolithic SEC column (250 mm × 5 mm).

Table 12
Summary of functional monomers used for monolith grafting and grafting yields (expressed in mmol monomer/g monolith)

Functional monomer	Capacity (mmol/g)
(norbornene dicarboxylic acid, COOH / COOH)	0.2
(norbornene methyl carboxylic acid, COOH)	0.14
(norbornene imide, valine, N-(3-nitrophenyl) amide, NO$_2$)	0.03
(N-phenyl norbornene dicarboximide)	0.22
(N-(4-hydroxyphenyl) norbornene dicarboximide, OH)	0.06
(N-(4-dimethylaminophenyl) norbornene dicarboximide, NMe$_2$)	0.26
(norbornene carboxylic ester, cyclodextrin)	n.d.
(norbornene carboxylic ester, cyclodextrin)	n.d.

applications and the quality of separations give an impressive demonstration of the capabilities of these new supports.

Acknowledgements

References

[1] M.R. Buchmeiser, J. Chromatogr. A 918 (2) (2001) 233.
[2] S. Penczek, P. Kubisa, R. Szymanski, Makromol. Chem. Rapid Commun. 12 (1991) 77.
[3] K. Matyjaszewski, Macromolecules 26 (1993) 1787.
[4] R.R. Schrock, Acc. Chem. Res. 23 (1990) 158.
[5] R.R. Schrock, Polyhedron 14 (1995) 3177.
[6] R.R. Schrock, A.H. Hoveyda, Angew. Chem. 115 (2003) 4740.
[7] R.R. Schrock, Chem. Rev. 102 (2002) 14.
[8] R.R. Schrock, J. Chem. Soc., Dalton Trans. (2001) 2541.
[9] P. Schwab, R.H. Grubbs, J.W. Ziller, J. Am. Chem. Soc. 118 (1996) 100.
[10] P. Schwab, M.B. France, J.W. Ziller, R.H. Grubbs, Angew. Chem. 107 (1995) 2179.
[11] R.H. Grubbs, B.M. Novak, D.M. McGrath, A. Benedicto, M. France, S.T. Nguyen, Polym. Prepr. (Am. Chem. Soc., Div. Polym. Chem.) 33 (1992) 1225.
[12] S.T. Nguyen, R.H. Grubbs, J. Am. Chem. Soc. 115 (1993) 9858.
[13] M.B. France, R.H. Grubbs, D.V. McGrath, R.A. Paciello, Macromolecules 26 (1993) 4742.
[14] R.H. Grubbs, J. Macromol. Sci., Pure Appl. Chem. A31 (1994) 1829.
[15] M.R. Buchmeiser, Chem. Rev. 100 (2000) 1565.
[16] R.H. Grubbs, in: R.H. Grubbs (Ed.), Handbook of Metathesis, Wiley-VCH, Weinheim, 2003.
[17] T.-L. Choi, R.H. Grubbs, Angew. Chem. 115 (2003) 1785.
[18] J.S. Fritz, P.J. Dumont, L.W. Schmidt, J. Chromatogr. A 691 (1995) 133.
[19] L.A. Berrueta, B. Gallo, F. Vicente, Chromatographia 40 (1995) 474.
[20] M.R. Buchmeiser, F. Sinner, R. Tessadri, G.K. Bonn, Austrian Pat. Appl., AT 405 056B (010497).
[21] M.R. Buchmeiser, N. Atzl, G.K. Bonn, Int. Pat. Appl., AT 404 099 (181296), PCT /AT97/00278.
[22] M.R. Buchmeiser, R. Tessadri, Austrian Pat. Appl., A 1132/97 (020797).
[23] M.R. Buchmeiser, N. Atzl, G.K. Bonn, J. Am. Chem. Soc. 119 (1997) 9166.
[24] I. Halász, K. Martin, Ber. Bunsen-Ges. Phys. Chem. 79 (1975) 731.
[25] I. Halász, K. Martin, Angew. Chem. 90 (1978) 954.
[26] G. Seeber, M.R. Buchmeiser, G.K. Bonn, T. Bertsch, J. Chromatogr. A 809 (1998) 121.
[27] D. Ambrose, J.S. Fritz, M.R. Buchmeiser, N. Atzl, G.K. Bonn, J. Chromatogr. A 786 (1997) 259.
[28] K. Eder, M.R. Buchmeiser, G.K. Bonn, J. Chromatogr. A 810 (1998) 43.
[29] C.G. Huber, M.R. Buchmeiser, Anal. Chem. 70 (1998) 5288.
[30] M.R. Buchmeiser, R. Tessadri, G. Seeber, G.K. Bonn, Anal. Chem. 70 (1998) 2130.
[31] M.E. Lipschutz, S.F. Wolf, J.M. Hanchar, F.B. Culp, Anal. Chem. 71 (1999) 1R.
[32] I. Jarvis, K.E. Jarvis, Chem. Geol. 95 (1992) 1.
[33] J.G. Crock, F.E. Lichte, T.R. Wildeman, Chem. Geol. 45 (1984) 149.
[34] J.G. Crock, F.E. Lichte, G.O. Riddle, C.L. Beech, Talanta 33 (1986) 601.
[35] R.M. Cassidy, Chem. Geol. 67 (1988) 185.
[36] S.J. Juras, C.J. Hickson, S.J. Horsky, C.I. Godwin, W.H. Mathews, Chem. Geol. 64 (1987) 143.
[37] M. Totland, I. Jarvis, K.E. Jarvis, Chem. Geol. 95 (1992) 35.
[38] F. Sinner, M.R. Buchmeiser, R. Tessadri, M. Mupa, K. Wurst, G.K. Bonn, J. Am. Chem. Soc. 120 (1998) 2790.
[39] M.R. Buchmeiser, M. Mupa, G. Seeber, G.K. Bonn, Chem. Mater. 11 (1999) 1533.
[40] R.M. Cassidy, S. Elchuk, Anal. Chem. 54 (1982) 1558.
[41] P. Kolla, J. Köhler, G. Schomburg, Chromatographia 23 (1987) 465.
[42] A. Kurganov, O. Kuzmenko, V.A. Davankov, B. Eray, K.K. Unger, U. Trüdinger, J. Chromatogr. 506 (1990) 391.
[43] M. Rätzsch, Prog. Polym. Sci. 13 (1988) 277.
[44] H. Engelhardt, H. Löw, W. Götzinger, J. Chromatogr. 554 (1991) 371.
[45] C.W. Huck, M.R. Buchmeiser, G.K. Bonn, J. Chromatogr. A 941 (2001) 33.

[46] M.R. Buchmeiser, G. Seeber, R. Tessadri, Anal. Chem. 72 (2000) 2595.
[47] G. Seeber, P. Brunner, M.R. Buchmeiser, G.K. Bonn, J. Chromatogr. A 848 (1999) 193.
[48] I. Glatz, M. Mayr, R. Hoogenboom, U.S. Schubert, M.R. Buchmeiser, J. Chromatogr. A 1015 (2003) 65.
[49] M.R. Buchmeiser, F.M. Sinner, PCT, A 604/99 (070499), PCT/EP00/02 846, WO 00/61288.
[50] R.C. Schulz, H. Waniczek, in: H. Bartl, J. Falbe (Eds.), Macromolecular Materials, Georg Thieme Verlag, Stuttgart, 1987, p. 608.
[51] S. Itsuno, K. Uchikoshi, K. Ito, J. Am. Chem. Soc. 112 (1990) 8187.
[52] K.B. Yoon, J.K. Kochi, J. Chem. Soc., Chem. Commun (1987) 1013.
[53] B. Mayr, M.R. Buchmeiser, J. Chromatogr. A 907 (2001) 73.
[54] M.R. Buchmeiser, F. Sinner, M. Mupa, K. Wurst, Macromolecules 33 (2000) 32.
[55] B. Mayr, F. Sinner, M.R. Buchmeiser, J. Chromatogr. A 907 (2001) 47.
[56] B. Mayr, H. Schottenberger, O. Elsner, M.R. Buchmeiser, J. Chromatogr. A 973 (2002) 115.
[57] K. Eder, E. Reichel, H. Schottenberger, C.G. Huber, M.R. Buchmeiser, Macromolecules 34 (2001) 4334.
[58] C.G. Huber, E. Stimpfl, P.J. Oefner, G.K. Bonn, LC–GC 14 (1996) 114.
[59] M.R. Buchmeiser, Macromol. Rapid. Commun. 22 (2001) 1081.
[60] M.R. Buchmeiser, F. Sinner, European Pat. Appl., 409 095 (A 960/99, 310599), PCT/EP00/04 768, WO 00/73782 A1, EP 1 190244 B1.
[61] N.B. Afeyan, N.F. Gordon, I. Mazsaroff, L. Varady, S.P. Fulton, Y.B. Yang, F.E. Regnier, J. Chromatogr. 519 (1990) 1.

[62] N.B. Afeyan, S.P. Fulton, F.E. Regnier, J. Chromatogr. 544 (1991) 267.
[63] A.E. Rodrigues, J. Chromatogr. B 699 (1997) 47.
[64] Y. Xu, A.I. Liapis, J. Chromatogr. A 724 (1996) 13.
[65] F. Sinner, M.R. Buchmeiser, Angew. Chem. 112 (2000) 1491.
[66] J.H. Knox, H.P. Scott, J. Chromatogr. 316 (1984) 311.
[67] J.H. Knox, H.J. Ritchie, J. Chromatogr. 387 (1987) 65.
[68] F. Sinner, M.R. Buchmeiser, Macromolecules 33 (2000) 5777.
[69] B. Mayr, R. Tessadri, E. Post, M.R. Buchmeiser, Anal. Chem. 73 (2001) 4071.
[70] S. Lubbad, B. Mayr, C.G. Huber, M.R. Buchmeiser, J. Chromatogr. A 959 (2002) 121.
[71] D. Liang, L. Song, Z. Chen, B. Chu, J. Chromatogr. A 931 (2001) 163.
[72] B. Mayr, G. Hölzl, K. Eder, M.R. Buchmeiser, C.G. Huber, Anal. Chem. 74 (2002) 6080.
[73] S. Lubbad, M.R. Buchmeiser, Macromol. Rapid Commun. 23 (2002) 617.
[74] M.R. Buchmeiser, S. Lubbad, M. Mayr, K. Wurst, Inorg. Chim. Acta 345 (2003) 145.
[75] E.C. Peters, F. Svec, J.M.J. Fréchet, Adv. Mater. 11 (1999) 1169.
[76] S. Lubbad, M.R. Buchmeiser, Macromol. Rapid Commun. 24 (2003) 580.
[77] M.R. Buchmeiser, G.K. Bonn, Am. Lab. 11 (1998) 16.
[78] M. Kolb, A. Bahr, S. Hippich, W. Schulz, Acta Hydrochim. Hydrobiol. 21 (1993) 308.
[79] H. Engelhardt, H. Löw, W. Eberhardt, M. Mauß, Chromatographia 27 (1989) 535.